

M.Sc. Eng. Sergiusz Łuczak,
Institute of Micromechanics and Photonics, Warsaw University of Technology
Dipl.-Ing. Stefan Reißner, Prof. Dr. rer. nat. Stephanus Büttgenbach,
Institute for Microtechnology, Technical University of Braunschweig (Germany)

TILT SENSOR BASED ON A 3-AXIS MEMS ACCELEROMETER

In the paper, one considers a possibility of using a three-axis monolithic MEMS accelerometer as a dual-axis tilt sensor to be applied as a microrobot equipment. The paper describes the sensor as well as results of the experimental studies performed on it in order to verify its usability, as far as the above application is concerned.

1. INTRODUCTION

Building mobile robots having miniature dimensions would be impossible unless there were devices featuring small overall dimensions that could be applied as their equipment. An example is a work on building a snake-like microrobot carried out in the Institute of Micromechanics and Photonics, Warsaw University of Technology [1]. The microrobot had to be equipped with a tilt sensor featuring miniature overall dimensions. Additionally, it had to detect both the roll and the pitch angles over the range of 360° with accuracy of indications of a few degrees arc.

It has been found out that in this case the most convenient solution is to build a tilt sensor employing measurement of gravitational acceleration, which can be transformed into tilt angles. The requirement of keeping miniature dimensions of the sensor favours the accelerometers fabricated in MEMS (Microelectromechanical Systems) technology.

Since it is required to measure both roll and pitch angles, two accelerometers are needed. However, because of the requirement of ensuring the accuracy of indications of the sensor of a few degrees arc, at least three accelerometers must be applied [2].

Most of the MEMS accelerometers have only one sensitive axis, few have two axes. So, the considered tilt sensor would consist of 3 or 2 accelerometers, what would result in increased overall dimensions. However, in the Institute for Microtechnology, Technical University of Braunschweig, an accelerometer has been designed and fabricated which features three sensitive axes in one chip. Hence, using the accelerometer for tilt measurement is the most convenient solution. It meets the first two requirements (i.e. miniature dimensions and dual-axis tilt measurement). The third requirement connected with its accuracy had to be checked out experimentally.

2. THE CAPACITIVE LOW-G 3D ACCELEROMETER

We used a micromechanical accelerometer which is capable of measuring the three components of the acceleration vector with only one sensor-chip. The chip is made by bulk-micromachining of single-crystalline silicon. It features four spring-mass systems which are used to detect acceleration-induced forces.

A seismic mass is the basic structure of the accelerometer. Each mass is suspended on two beams which serve as a spring. This structure is manufactured by anisotropic wet etching of <100>-oriented silicon wafers.

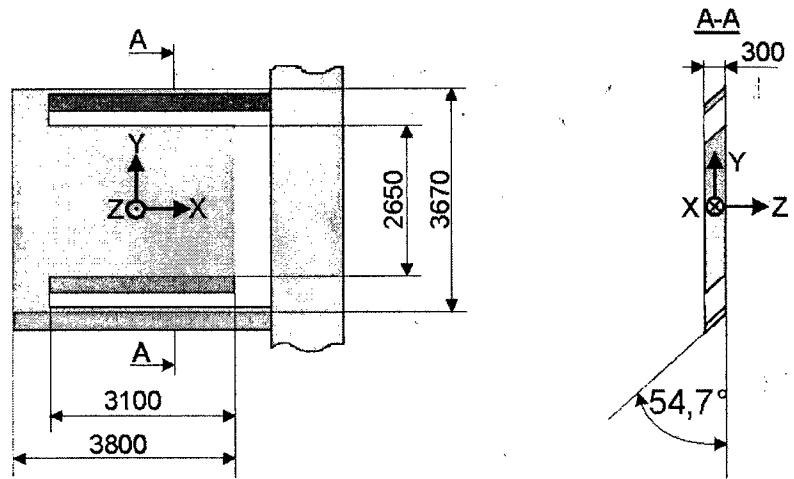


Fig. 1. The basic silicon structure (all dimensions are given in μm)

The beams which suspend the mass make an angle of 54.7° with the wafer surface. This angle is achieved owing to a special etching technology. The deflection of the mass takes place only in orthogonal direction with respect to the beams. Therefore, each mass is sensitive to acceleration in two of the three cartesian directions x , y , z (as denoted in fig. 2). One sensor contains four of the structures shown in fig. 1, each one rotated by 90° (fig. 2).

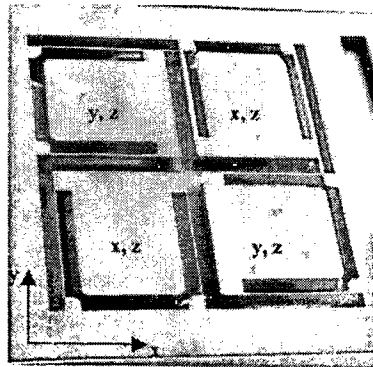


Fig. 2. The silicon die with four seismic masses

The four masses, which are suspended on differently oriented beams, enable detection of the three components of the acceleration vector [3]. The silicon die is assembled with two pyrex-glass covers to enable a capacitive readout. The pyrex covers provide cavities, so that a differential capacitor is formed for each of the four channels (fig. 3).

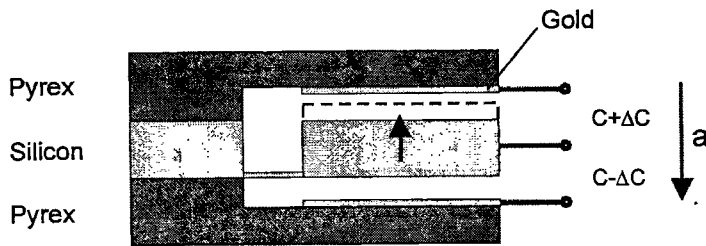


Fig. 3. One of the four differential capacitors

As shown in figure 3, acceleration causes a displacement of the seismic mass which is also the middle electrode of the differential capacitor. Thus, the capacities of the upper and lower capacitor change. While acceleration of ± 1 g is applied, the capacities change within a range from 19.3 pF to 19.8 pF.

3. THE ELECTRONIC EVALUATION CIRCUIT

To evaluate the deflection of one seismic mass, the belonging capacities must be measured. The voltage on a capacitor is given by:

$$U = \frac{Q}{C} \quad (1)$$

where Q is the charge and C is the capacity. The charge is defined as:

$$Q = \int I \cdot dt \quad (2)$$

where I is the charging current. If the capacitor is loaded with a constant current equation (2) is reduced to:

$$Q = I \cdot t \quad (3)$$

Thus, with a constant current and a constant charging time, the voltage on the capacitor indicates the capacity as shown in equation (4).

$$U = I \cdot t \cdot \frac{1}{C} = \text{const} \cdot \frac{1}{C} \quad (4)$$

We connect the moveable middle electrode of the differential capacitor to ground, and we use equation (4) to evaluate the two capacities. The upper and lower capacitors are cyclically loaded with a constant current and then unloaded at a frequency of about 80 kHz. Courses of the voltages $U_1(t)$ and $U_2(t)$ on the capacitors are shown in fig. 4.

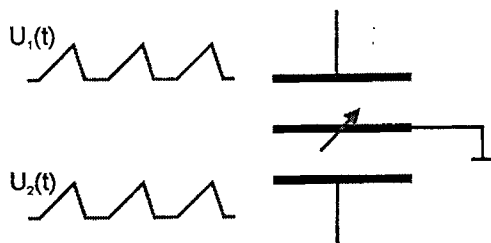


Fig. 4. Operation principle of the evaluation circuit

The peak values U_{1max} and U_{2max} of these voltages, being dependent on the values of the capacities, are compared and then amplified into an output voltage U_{OUT} which is proportional to the position of the middle electrode, and varies within a range from 0 to about 4 V (fig 5). A more sophisticated evaluation method for differential capacitors, using a compensated, so called 'closed loop' evaluation principle, is described in [4].

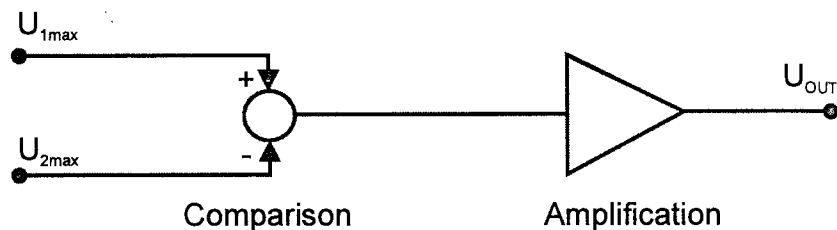


Fig. 5. The CAV414 circuit used for evaluation of one channel of the sensor chip

A photograph of the evaluation circuit coupled with the sensor is shown in fig. 6. The evaluation circuit provides four output channels which evaluate the positions of the four seismic masses. The dimensions of the circuit are 78mm x 45mm, and of the sensor itself 13mm x 13mm x 2mm.

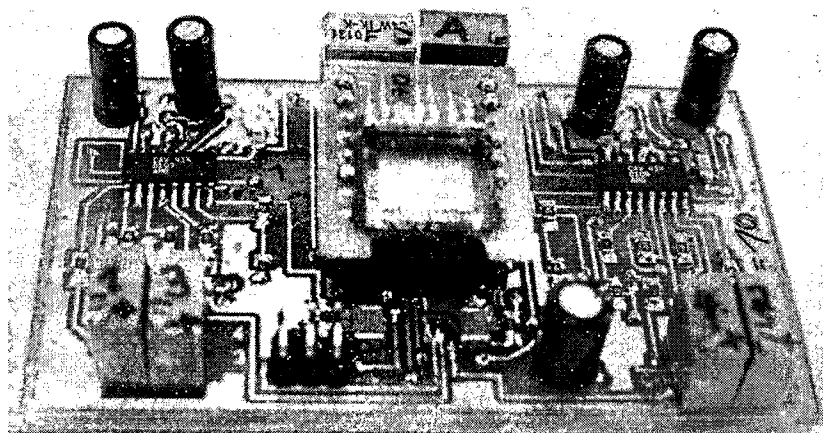


Fig. 6. Evaluation circuit with the sensor-chip (in the middle)

4. THE EXPERIMENTAL STUDIES

In order to carry out the experimental studies on the accelerometer, a special computer controlled test station has been used [2]. Its principle of operation is as follows. The computer sets a certain angular position of the tested accelerometer (i.e. certain pitch and roll angles) and then reads its output signals. This way, we can obtain indications of the tested sensor against the corresponding real angular positions. Comparison of these two provides information on the sensor accuracy.

The tests were performed in the following way. First, a desired angular position was applied and then, after a time of few seconds - to damp vibrations of the sensor, 30

readouts of the output signals were performed (at the same angular position). The procedure was repeated until all the desired angular positions were reached.

The results presented below were computed on the basis of average values of the 30 accelerometer readouts. In the case of using a single readout, the maximal values of the errors would be higher.

4.1. Accuracy of applying the angular position

It is usually assumed that the accuracy of the measuring device is to be 10 times higher than the expected accuracy of the quantity to be measured. Accuracy of applying the roll angle was of $\pm 0.04^\circ$, and of the pitch angle $\pm 0.03^\circ$ (for the roll angle of 0°). Thus, tilt angles having indication accuracy no higher than $\pm 0.4^\circ$ could be measured. The above condition was fulfilled since the considered accuracy was lower, as presented below.

4.2. Accuracy of reading the output signals from the accelerometer

Accuracy of measuring the output voltages from the electronic circuit coupled with the accelerometer results from the accuracy of the applied analog-digital data acquisition card (Advantech PCL - 818 L) and was no lower than 0.022 V.

5. RESULTS OF THE EXPERIMENTAL STUDIES

Because of a high number of the obtained results, the paper presents only some of them. Since all the four channels operate analogously, only one of them (channel #2) was chosen for further testing.

5.1. Characteristic of the sensor

In Fig. 7 a characteristic of the sensor is presented. It was obtained while applying the pitch angle with a step of 5° , by a constant roll angle (of -180°). Course of the signal is according to the expected one (i.e. sine function [5]).

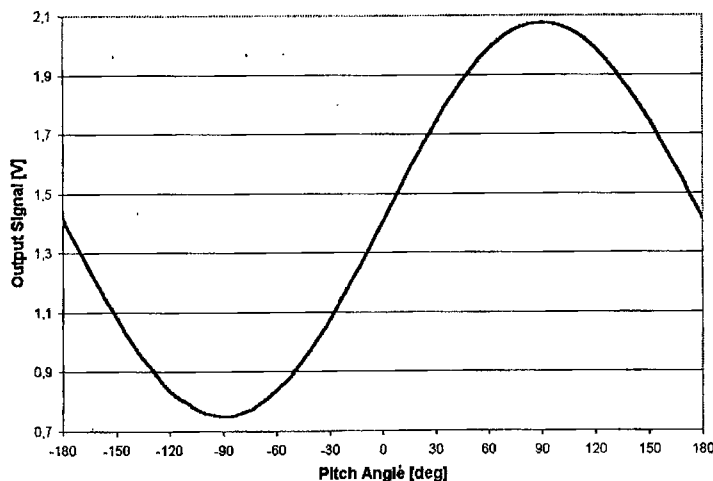


Fig. 7. Characteristic of the sensor while pitched

5.2. Calibration of the sensor

In order to determine the value of a measured tilt angle, the accelerometer must be calibrated first. The calibration process is meant to determine 2 constants for each sensitive axis of the accelerometer:

- the offset voltage - i.e. voltage corresponding to a position where the roll and the pitch angles are of 0° (with respect to the position of the sensitive axis),
- sensitivity of the accelerometer, i.e. amplitude of variations of the output voltage corresponding to variations of the tilt angle over the round angle (i.e. $-180^\circ \div 180^\circ$).

Additionally, a phase shift (a shift between the sensor characteristic and the tilt angles indicated by the test station) must be determined. All the three constants can be obtained by means of a nonlinear regression described as

$$V = V_s \sin(\alpha + \varphi) + V_o \quad (5)$$

where V is the actual output voltage, V_s the sensitivity of the active axis, α the pitch angle, φ the phase shift, and V_o the offset voltage.

For all of the regressions used in the further computations, the adjusted R-Squared statistic was over 99.99%, what indicated that the models fitted very well the variability of the output voltages. All the estimates (i.e. the determined calibration constants) were statistically significant (for the accepted confidence level of 95%).

5.3. Errors of the sensor indications

Having calibrated the accelerometer, it was possible to compare its indications with the real angular positions applied by means of the test station. In order to do this, the pitch angle was computed applying the following formula (resulting from (5))

$$\alpha = \arcsin \frac{V - V_o}{K_s} - \varphi = \arcsin V_c - \varphi \quad (6)$$

where V_c is a calibrated variable. Because of the fact that the absolute value of the calibrated variable can slightly exceed 1 (and thus be out of the domain of the arcsine function), the following formula was applied when this was the case

$$V'_c = \frac{V_c}{|V_c|} (2 - |V_c|) \quad (7)$$

and then, V_c in formula (6) was replaced with the new V'_c . The above transformation was based on the fact that for an error to have a negative value is equally probable as to have a positive value.

Fig. 8 presents the total error of the accelerometer indications presented in fig. 7. The error is meant as a difference between the real angular position of the sensor (applied by means of the test station) and the position calculated according to (6). There are presented two courses - one for the roll angle of 180° (dashed line) and the other for the roll angle of 0° (solid line).

Fig. 9 presents the total error of the accelerometer indications for a characteristic obtained analogously to the one presented in fig. 7 - applying the roll angle with a step of 5° , by a constant pitch angle of 0° . The error is defined as in fig. 8. The limited range of the roll angle ($-235^\circ \div 55^\circ$) resulted from technical reasons. While obtaining the characteristic, the sensor was attached to the test station as described in section 5.4.

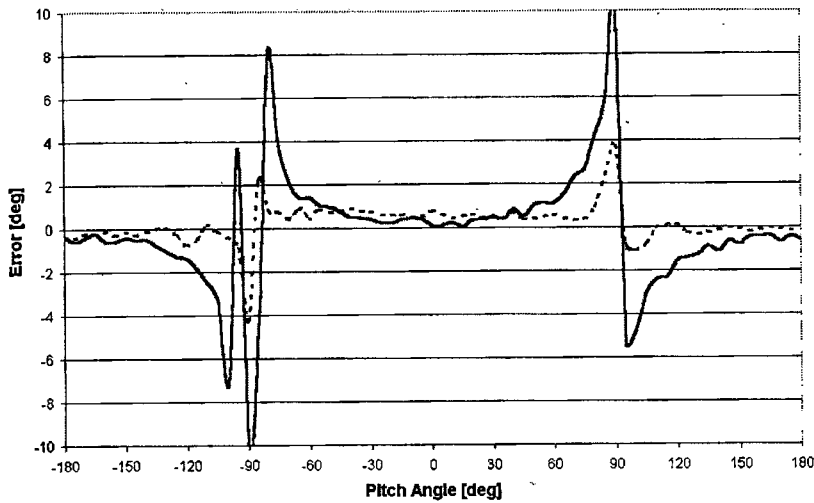


Fig. 8. Total indication error of the sensor while pitched

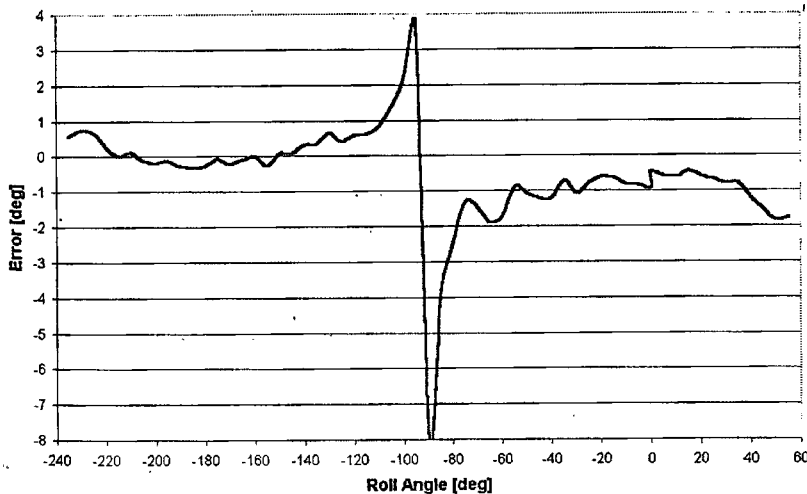


Fig. 9. Total indication error of the sensor while rolled

As can be observed, both courses of the indication errors presented in fig. 8 and 9 are similar as far as their shape and the error values are concerned. A rapid increase of the indication errors can be observed in both cases for tilt angles of ca. -90° , while in other regions they are usually of about $1^\circ \div 2^\circ$. The increase results from insensitivity of the sensor within this angular region due to flatness of its characteristic (see fig. 7).

5.4. The transverse sensitivity of the sensor

In order to determine the transverse sensitivity of the sensor, it was attached to the test station in such a way, that its sensitive axis (i.e. axis of channel #2) overlapped the pitch axis of the test station. This was obtained in an experimental way by aligning the sensor

position around the roll- and z-axis, and finding a position where the amplitude of variations of the output voltages had the lowest value while pitching the sensor.

The transverse sensitivity was tested in the following way. By means of the test station various pitch angles were applied (within the range of $-180^{\circ} \div 180^{\circ}$ with a step of 30°), and then the sensor was rolled (within a limited, due to some technical limitations, range of $-185^{\circ} \div 15^{\circ}$). This way, there were obtained characteristics like in fig. 7, and then the total error of the sensor indications for each characteristic was determined. Results are presented in fig. 10.

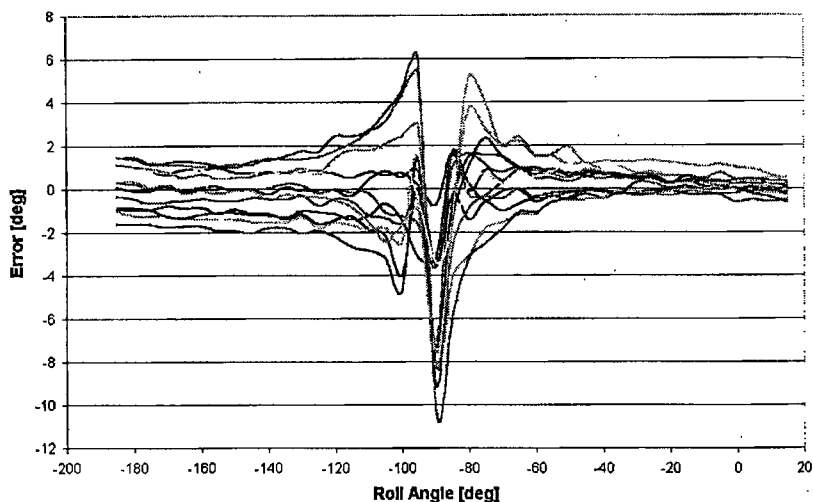


Fig. 10. Courses of the total error of the roll indications for various pitch angles

Again, as can be clearly observed, the above courses resemble the ones presented before. Some influence of the pitch angle can be observed, but it does not significantly change the metrological features of the sensor.

5.5. Hysteresis of the sensor

In order to detect hysteresis of the sensor, the test station was equipped with an incremental angle transducer. Thus, the accuracy of applying the roll angle was of about 0.0006° . There were obtained two characteristics while rolling the sensor by the pitch angle of about 0° - one for clockwise rolling, and the other for counterclockwise rolling. However, no significant influence of the direction of rolling the sensor on its indications was observed. This may be explained by the fact that the hysteresis loop is of a very small value, and that the seismic mass is vibrating while changing position of the sensor, so the direction of rotation does not matter.

5.6. Random errors of the sensor

Random errors of tilt indications were independent on the sensor position. Their values, meant as a 3-sigma error, were usually of 0.001 V for an average indication and of 0.007 V for a single indication. These values correspond to various errors of a tilt angle, dependently on its value (e.g. 0.001 V causes an error of 0.1° for the pitch or roll angle of 55°).

6. DUAL-AXIS TILT MEASUREMENT

In Fig. 8-10, it can be observed that the total indication error dramatically increases around the roll (and analogously the pitch) angle of $\pm 90^\circ$. This reveals the main disadvantage of using accelerometers for tilt measurement - their strongly nonlinear characteristic in this application (see fig. 7).

However, because of the fact that the tested accelerometer has 4 sensitive axes, the regions of insensitivity (around the roll and pitch angles of $\pm 90^\circ$) can be omitted owing to specific calculation [5]. Here, in order to make use of the mentioned calculation (meant for 3 sensitive axes forming cartesian x - y - z -axis), the spatial configuration of the sensitive axes of the accelerometer must be additionally taken into account. The component accelerations must be transformed into cartesian components, using e.g. formulae given in [3]. That transformation will not decrease accuracy of determining the tilt angles, since the angle between the sensitive axes is defined very precisely, as resulting from crystallographic features of the silicon. Additionally, it should be noted that it is enough to have only 3 components (not necessary in a cartesian co-ordinate system) of a vector in order to determine its orientation.

Thus, not all indications are needed to determine the tilt angles (i.e. pitch and roll). There are two sensitive axes within the xz plane and two axes within the yz plane, all rotated by 54.7° with respect to the vertical. In this case, indications on each sensitive axis within a range of $\pm 55^\circ$ (and 125° - 235°) are sufficient, for when the tilt angle exceeds this range for an axis, indications of the adjacent axis can be used (for which the tilt angle just enters the range of $\pm 55^\circ$). In the case of having an accelerometer with three sensitive axes forming cartesian x - y - z -axis, this range would be smaller - of $\pm 45^\circ$. The above considerations are also true for single-axis tilt measurement, when only two sensitive axes (contained within the same vertical plane) are needed.

Applying the above methodology, the accuracy of the studied accelerometer can be evaluated as no lower than 2° (see fig. 8-10), what is quite satisfactory, taking into account that the measuring range is of 360° for each tilt axis.

7. CONCLUSIONS

The works carried out proved that it is possible to use the presented MEMS accelerometer as a dual-axis tilt sensor that meets the requirements described in the first section. However, there must be applied certain processing of the output data in order to ensure satisfactory accuracy of the tilt indications.

There have been obtained values of such metrological features of the sensor as the total accuracy of tilt measurement (of ca. 2°) and random errors (of ca. 0.1° for the tilt angle of 55°).

Dynamic properties of the sensor have not been studied because of the type of its application (i.e. as a tilt sensor operating only under static, or quasi-static conditions).

Owing to suspending the seismic mass on two springs, the transverse sensitivity of the sensor is insignificant. Even though there can be observed some differences in courses of the indication errors for various pitch angles (see fig. 10), they should be rather ascribed to an unavoidable residual misalignment of the sensor in the test station and other errors of a random character. Featuring insignificant transverse sensitivity is very

important, since it is in a large measure a source of indication errors in the case of some other MEMS accelerometers.

7.1. Future works

The regression constants (see formula (6)) were determined separately for the courses whose errors are presented in fig 8, 9 and 10. The reason for this was the fact that the offset voltage drifted significantly during the tests.

Therefore, the future works should be focused on designing better electronic circuits processing the sensor signals. The emphasis should be put especially on decreasing the drift of the offset voltage (caused mainly by temperature variations).

The best solution would be to fabricate the whole evaluation unit as an integrated circuit. This would result in small dimensions of the unit as well as increasing accuracy of the sensor.

8. ACKNOWLEDGEMENTS

The experimental studies have been supported by the Polish State Committee for Scientific Research (grant No. 5 T07C 040 22).

REFERENCES

- [1] W. Czerwiec, W. Oleksiuk: *Mini-Robot Designed for Moving Inside of Pipes*; Conference *Computer Simulation in Machine Design*, Wierzba, 2000, Proc. pp. 103-110
- [2] S. Łuczak: *MEMS Tilt Sensor for Microrobots*; Conference *Automation 2002*, Warsaw, 2002, Proc. pp. 339-346
- [3] S. Bütefisch, A. Schoft, S. Büttgenbach: *Three-Axes Monolithic Silicon Low-g Accelerometer*; *Journal of Microelectromechanical Systems*, Vol. 9, No. 4, 2000, pp. 551-556
- [4] S. Beissner, M. Puppich, S. Bütefisch, S. Büttgenbach, T. Elbel: *Analog Force Feedback Circuit for Capacitive Micromechanical Acceleration Sensors*; 10th International Conference *Sensor 2001*, Nuremberg (Germany), 2001, Proc. Vol. 2 pp. 577-582
- [5] S. Łuczak: *Standard MEMS Accelerometer as a Dual-Axis Tilt Sensor*; Conference *47 Internationales Wissenschaftliches Kolloquim*, Ilmenau (Germany), 2002, Proc. pp. 244-245 & CD ROM